JOURNAL OF COMPUTATIONAL PHYSICS 28, 43–55 (1978)

A Monte Carlo Algorithm for Calculating Neutral Gas Transport in Cylindrical Plasmas

M. H. HUGHES* AND D. E. POST

Princeton University Plasma Physics Laboratory, Princeton, New Jersey 08540

Received March 22, 1977; revised August 23, 1977

Monte Carlo techniques have been used to calculate neutral gas distributions in tokamaks. The algorithm uses track length estimators, suppression of absorption, and splitting with Russian roulette to reduce the variance, so that the algorithm is economic. The resultant package is small in memory requirements and relatively fast (~15 seconds of PDP-10 KI time per neutral density profile). The tokamak is modeled as an infinite cylinder, and the plasma parameters are specified as a function of the radial coordinate of the cylinder. The effects of wall reflection and sputtering yields can be easily computed within the model. The algorithm has been incorporated in a one-dimensional tokamak transport code. The code has also been used to predict the energy spectra of charge-exchange neutrals which form the basis for measurements of ion temperatures in tokamaks.

1. INTRODUCTION

The interaction between the plasma and recycling neutral gas is an important feature of any tokamak model. For example, the presence of a neutral species in a plasma influences both the particle and energy balance while energetic neutrals produced in successive charge exchange collisions can carry energy directly to the walls and sputter heavy impurity atoms back into the discharge. Further, it has been suggested [1] that the reflection of escaping particles as high-energy neutrals is an important mechanism in producing high-density tokamak discharges by gas injection.

To study such effects in detail, an accurate treatment of the neutral gas is required. Here, we describe a Monte Carlo approach to the problem. The model is implemented in a code which provides a flexible and convenient framework for developing numerous physics calculations dependent on the neutral population in a plasma. The package itself is sufficiently fast and compact to be incorporated, for example, as part of a one-dimensional radial plasma transport code.

2. MONTE CARLO METHOD

Neutral gas transport is, in principle, similar to the problem of neutral transport; in fact, it has been advocated [2] that neutron codes should be adapted to calculate neutral behavior. However, neutral atoms traversing a plasma are subject only to

* On leave from UKAEA, Culham Laboratory, Abingdon, United Kingdom.

0021-9991/78/0281-0043$02.00/0

ionization and charge exchange for which the cross sections are smooth functions free from troublesome resonances. The Monte Carlo technique is then much more straightforward. The computational scheme described here will determine, with adequate statistical accuracy, the neutral density and energy distributions within a plasma. The method works satisfactorily with relatively few simulated particles (typically $\lesssim 10^3$) even in situations involving deep penetration to the center (e.g., where the neutral density is attenuated by factors $\sim 10^4$–10^5).

2.1. *Analog Method*

From an elementary argument, it is easily shown that the distance l, which a neutral particle traverses between collisions is given [3] by

$$\int_0^l \frac{ds}{\lambda} = -\ln \xi \tag{2.10}$$

where λ is the local mean free path and ξ is a random number in the range $0 \leqslant \xi < 1$. The integral is evaluated along the directed straight line from one collision to the next. Since a plasma is an inhomogeneous medium, we invert Eq. (2.10) by dividing the plasma volume into zones in which the density and temperature are piecewise homogeneous. The distance to a collision is then obtained by calculating the lengths $s_1, s_2, s_3, \ldots, s_N$ of the segments which lie in each zone. If

$$\sum_{j=1}^{n-1} \frac{s_j}{\lambda_j} \leqslant -\ln \xi < \sum_{j=1}^{n} \frac{s_j}{\lambda_j}, \tag{2.11}$$

then the trajectory ends in the nth zone a distance

$$\delta_n = \lambda_n \cdot \left(-\ln \xi - \sum_{j=1}^{n-1} \frac{s_j}{\lambda_j}\right) \tag{2.12}$$

beyond the entrance to the nth region.

Since the path of motion of a neutral atom is a straight line and the velocity is constant between collisions, particle tracking is particularly convenient in a Cartesian coordinate system. Thus, the distance s_j in Eq. (2.12) can be obtained from the intersections of the straight line

$$\mathbf{r} = \mathbf{r}_0 + \mathbf{v}(t - t_0) \tag{2.13}$$

and the equation $f_j(x, y, z) = 0$ of the jth boundary surface. Here $\mathbf{r}(t)$ is the particle position at time t, $\mathbf{r}_0$ the initial position (at $t = t_0$), and $\mathbf{v}$ is the particle velocity. In our present model, we consider a cylindrical plasma with concentric circular surfaces. The computation of the s_j's is then simply obtained from the solution of the equations:

$$x^2 + y^2 = a_j^2 \tag{2.14a}$$

and

$$\frac{x - x_0}{v_x} = \frac{y - y_0}{v_y} = \frac{z - z_0}{v_z} = t - t_0 \tag{2.14b}$$

where a_j is the radius of the jth surface.

The tracking of a particle is illustrated in Fig. 1. A particle is launched from the edge of the plasma at $(a, 0.0)$ and tracked to the first collision. There it is scattered and is followed through successive collisions until it escapes or is ionized.

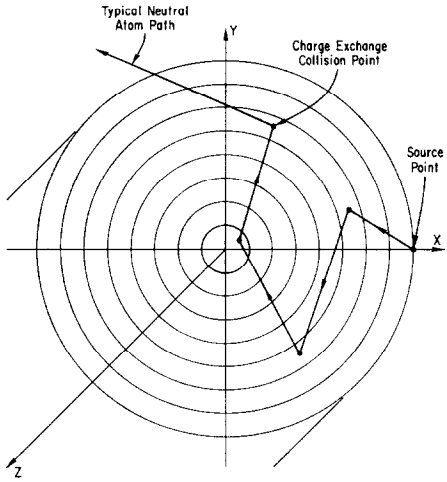

FIG. 1. Particle tracking geometry.

It is worth noting that the dimension along the z axis enters the problem only in the computation of v as $| \mathbf{v} | = (v_x^2 + v_y^2 + v_z^2)^{1/2}$.

2.2 *Scoring*

The neutral density in any zone j is obtained from a path length estimator [4], which can be written in the form

$$\bar{n}_j = \frac{\Gamma A}{V_j N} \sum_{i=1}^{N} \omega_i t_{ij} \,. \tag{2.20}$$

Here, Γ is the influx of neutrals across the plasma boundary, A is the total surface area of the plasma, V_j is the volume of zone j, N is the number of sample particles, ω_i is the statistical weight of particle i and t_{ij} is the time taken for particle i to traverse zone j. We also calculate the mean neutral temperature in zone j which is defined as

$$\bar{E}_j = \frac{2}{3} \sum_{i=1}^{N} \frac{1}{2} m v_i^2 \omega_i t_{ij} \Big/ \sum_{i=1}^{N} \omega_i t_{ij} \,. \tag{2.21}$$

The factor of 2/3 converts the mean energy to a "temperature" for comparison with the local ion temperature.

The path length estimator is an important part of the algorithm since a particle contributes information in each region through which it passes, rather than only at the point of collision.

2.3 *Suppression of Absorption*

In the simplest analog scheme, a particle launched at the boundary is tracked using Eqs. (2.10)–(2.14) until a collision point is found. The collision can either be an ionization or a charge exchange event. The probabilities for these two events are sampled by choosing a random number ξ uniformly distributed between 0 and 1. The probability of ionization is $p_{\text{ion}} = (1/\lambda_{\text{ion}})/(1/\lambda_{\text{cx}} + 1/\lambda_{\text{ion}})$. If $\xi < p_{\text{ion}}$, the particle is considered to be ionized and is lost. A new particle is launched at the boundary and the whole process is repeated again. If $\xi \geqslant p_{\text{ion}}$, the particle is considered to have undergone a charge exchange, and a new particle is launched from the point of collision. The velocity of the new particle is chosen from a Maxwellian distribution characterized by the local ion temperature. This procedure is repeated until the particle is lost by ionization or escapes from the system.

This simple method suffers from two main deficiencies. First, the sample particles are heavily attenuated by ionization in the outer region of the plasma; second, the zone volume decreases as particles penetrate toward the center of the plasma. Both effects reduce the number of particles which reach the center and increase the statistical error there.

We circumvent the first problem by suppressing absorption. This simply means that at a collision a sample particle is never lost by ionization. Instead, we reduce its weight ω by a factor $\lambda_T/\lambda_{\text{cx}}$ where λ_T is the total mean free path and continue tracking after selecting a new velocity as described above. This procedure continues until the particle either escapes or its weight drops to some prescribed minimum value $\omega_{\min}$. When $\omega \leqslant \omega_{\min}$, we revert to the simple analog scheme outlined above until the particle is lost.

2.4 *Splitting and Russian Roulette*

To reduce the variance caused by decreasing zone size, we use a splitting scheme as follows. At some prescribed boundaries $r = r_s$ within the plasma we split a sample particle with weight ω into ν identical particles each with weight ω/ν, provided that the particle is moving inwards toward the center of the plasma. Alternatively, if the particle is moving radially outwards across one of the surfaces r_s, then the particle is destroyed with probability $(1 - 1/\nu)$; if it survives, its weight is increased by a factor ν. The splitting parameters ν need not be an integer and may take different values on the surfaces r_s. Thus, if $n < \nu < n + 1$, we choose n particles with probability $(n + 1 - \nu)$ and $n + 1$ particles with probability $(\nu - n)$.

It is shown in Ref. [4] that this procedure does not alter the basic Monte Carlo game of chance. Now, however, a particle moving toward the center is multiplied

and the new particles are placed in a list to be picked up later. When the original particle is lost, each new particle is taken in turn from the list until it is lost, at the same time, creating even more particles. When there are no more particles left in the list, another source particle is selected. By judicious choice of splitting surfaces, we can maintain a roughly constant particle flux across the plasma radius and therefore reduce the number of source particles. Generally, we choose $\nu = 2$ and space the splitting boundaries so that the flux falls by half between them.

The combination of suppressing absorption and splitting with Russian roulette very effectively reduces the computer time required to calculate a set of neutral profiles. For example, the neutral package incorporated as part of the Princeton Plasma Physics Laboratory radial transport code BALDUR [5] typically employs 200 particles with 20 zones; the CPU time required to calculate the neutral profiles for PLT parameters is ~15–20 sec on a DEC-PDP 10 KI.

2.5 *Collision Cross Sections*

The calculations described here refer to H° atoms in a hydrogen plasma. We suppose that the ion temperature is sufficiently low that the dominant processes are charge-exchange and electron impact ionization of the neutral gas. The reaction rate, $\langle \sigma v \rangle_i$, for the latter process is obtained from the polynomial fit given in Ref. [6]. Since $\langle \sigma v \rangle_i$ is independent of the neutral velocity, this quantity is tabulated for each zone. On the other hand, the charge-exchange reaction rate depends on the neutral velocity and is calculated for each particle. The charge-exchange cross section is calculated from a formula given by Riviere [7], viz.,

$$\sigma_{cx} = \frac{0.6937 \times 10^{-14}[1 - 0.155 \log_{10}(E_{\text{rel}})]^2}{1 + 0.112 \times 10^{-14} E_{\text{rel}}^{3.3}}.$$

E_{rel} (eV) is computed from the root-mean-square velocities of the neutral atom and the background ions. The average speed of an ion with temperature T is $\bar{v} = (8kT/\pi m)^{1/2}$. The relative velocity can be defined as $v_{\text{rel}}^2 = v_0^2 + \bar{v}_{\text{ion}}^2$ where v_0 is the velocity of the neutral atom. Thus, $E_{\text{rel}} \equiv mv_{\text{rel}}^2/2 = mv_0^2/2 + 4kT/\pi$. Then, $\langle \sigma v \rangle_{\text{cx}}$ can be defined as $\sigma_{\text{cx}}(E_{\text{rel}})\, v_{\text{rel}}$. The exact form of E_{rel} and v_{rel} is relatively unimportant since for E_0, $T_i < 20$ keV, $\langle \sigma v \rangle_{\text{cx}}$ is almost independent of E_{rel}.

2.6 *Surface Interaction*

Energetic particles incident on a solid can penetrate the surface and have some probability, dependent on their energy, of being backscattered having deposited part of their energy in the material. At the same time, if the particles are sufficiently energetic, they can sputter material from the surface. The data available for calculating surface interactions have been summarized by Behrisch [8].

To calculate the flux of backscattered particles, we require the particle reflection coefficient $R(\epsilon)$ and the energy distribution $I(\epsilon)\, d\epsilon$ of reflected particles. For hydrogen atoms incident on stainless steel, this information is given in Ref. [8] in the form of histograms with broad energy ranges. Thus, in the Monte Carlo calculation, a particle

with energy ϵ' which escapes from the system is reflected with its weight reduced by $R(\epsilon')$ and a new energy ϵ obtained by inverting the equation

$$\int_0^{\epsilon} I(\epsilon)\, d\epsilon = \xi$$

where ξ is a random number in the range $0 \leqslant \xi < 1$. The angle of reflection, ϕ, is chosen from a cosine distribution viz. $\cos\phi\, d\Omega/2\pi$ where $d\Omega$ is the element of solid angle.

To calculate the flux of sputtered material, the sputtering coefficients given in Ref. [8] are tabulated from the threshold energy ($\sim$70 eV for protons incident on stainless steel) to 20 keV. Although the dependence of the sputtering yield on the angle of incidence, θ, is not well known, it is suggested [8] that the normal incidence value should be increased by $(\cos\theta)^{-f}$ with $1 < f < 2$; we have taken $f = 1$ with a cutoff at 80°. The sputtered flux is also assumed to have a cosine distribution.

2.7 *Neutral Source*

The external source of neutrals is an important consideration in this problem. We consider two models:

(a) a monoenergetic, isotropic source;
(b) neutralization and backscattering of outflowing protons.

Model (a) is widely used in transport codes and could arise from dissociation of H_2^+ produced by ionization of H_2 from the walls.

There is some experimental evidence that the limiter in a tokamak is an important source of neutral gas [10]. In model (b) we suppose that a proton incident on the limiter is neutralized and reflected as a neutral. Thus, we select particles from a Maxwellian distribution at the edge ion temperature and, using the backscattering model described previously, we calculate a reflection probability R for each particle together with a reflection angle and energy. The particle is then launched with weight R.

Note added in proof. The statistical weight of a particle launched from the edge representing a flux Γ should be $(v/v_0) \times \cos\beta$ where v is the actual particle velocity, v_0 is the average velocity of the distribution, and θ is the angle from the normal direction.

3. Illustrative Calculations

The code requires as input the distributions of electron and ion density and temperature. We present some typical calculations assuming:

$$n_e = n_i = 5 \times 10^{13}[1 - (r/a)^2]\ \text{cm}^{-3},$$
$$T_e = 2 \times 10^3[1 - (r/a)^2]\ \text{eV},$$
$$T_i = 1 \times 10^3[1 - (r/a)^2]\ \text{eV},$$

with a plasma radius, $a = 40$ cm. In each calculation, the incoming flux of neutrals is normalized so that the external density is the same (10^{10} cm^{-3}).

Figure 2 shows the neutral density and energy distributions arising from a monoenergetic (3 eV) source of cold gas assuming (a) perfectly absorbing surfaces and (b) the backscattering model described in Section 2.6. The change in the density distribution when backscattering is taken into account is relatively small; for example, the central density has increased from 1.4×10^7 to 2.2×10^7 cm^{-3}. The change in the energy distribution within the plasma is insignificant.

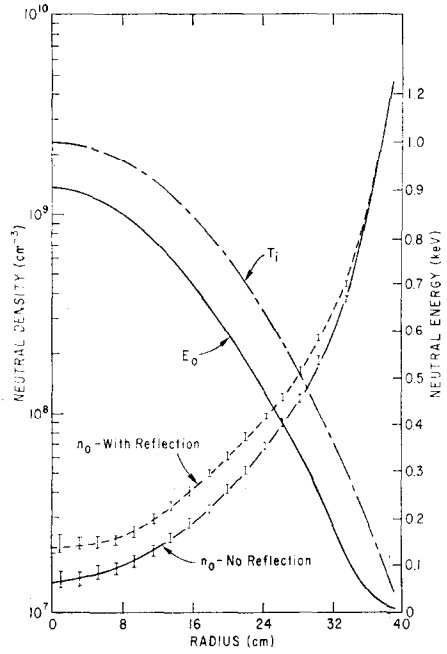

FIG. 2. Neutral density and energy distributions arising from a monoenergetic source ($E = 3$ eV).

The small effect of backscattering neutrals is due to the rapid decrease of the particle reflection coefficient with increasing energy [8]. Figure 3 illustrates the energy distributions of the escaping neutral flux $d\Gamma^+/d\epsilon$ and the reflected flux $d\Gamma^-/d\epsilon$. Thus while the distribution function of the escaping particles has a maximum at 60–80 eV (corresponding to the mean-ion energy $\sim$1 neutral mean free into the plasma) the distribution of reflected particles decreases rapidly from low energies; the ratio $\Gamma^-/\Gamma^+ \sim 0.3$. The net result is that the mean energy of neutrals crossing the plasma boundary is increased from 3 to 6 eV.

Figure 4 shows the neutral profiles arising from the alternative boundary model (b) of Section 2.7. In this case we suppose that protons with *temperature* 30 eV are incident on the limiter and are reflected as neutrals; the mean *energy* of the reflected particles is 17.4 eV. Again, reflection of escaping neutrals has only a small effect on the density distribution. Also shown in Fig. 4 for comparison is the distribution arising from a 17.4-eV monoenergetic source.

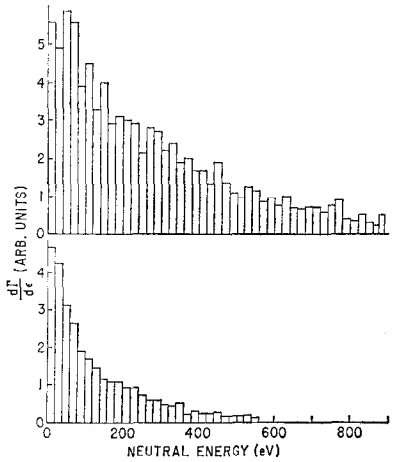

FIG. 3. (top) Energy distribution of escaping neutrals. (bottom) Energy distribution of reflected neutrals.

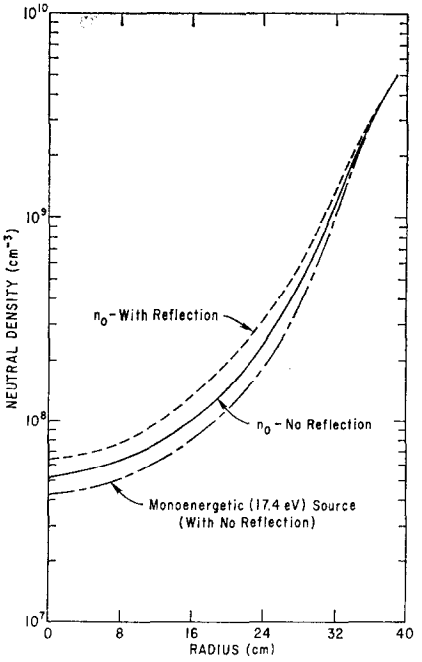

FIG. 4. Neutral density and energy distributions arising from a distributed source ($E = 17.4$ eV).

These results suggest that the high energies (50–100 eV) of incoming neutrals sometimes invoked in transport code calculations [9] are not justified unless the ion temtemperature near the limiter is extraordinarily high ($\gtrsim$100 eV).

3.1 *Comparison with Düchs' Code*

The Düchs–Rutherford 1D radial transport code [9] is used extensively for tokamak modeling. It is of some interest to compare the neutral treatment in that code with the present Monte Carlo model.

The Düchs' code includes an influx of cold gas at the plasma boundary together with 10 generations of hot neutrals produced in successive charge exchange collisions. At each charge-exchange event, the neutrals acquire the local-mean-ion energy but are constrained to move in the plane. Using the Monte Carlo code, we can simulate this model if, at each charge exchange collision, a neutral is given a new velocity corresponding to a mean-ion energy and its direction is chosen randomly in a disk; similarly when launching a particle its direction is confined to the plane. Figure 6 shows that in this case we can accurately reproduce the neutral density profile calculated by the Düchs code.

Also shown in Fig. 5 is the density distribution obtained if we remove the constraint of no axial motion and we select a new velocity at a collision from a Maxwellian distribution at the local ion temperature. In this case the density distribution decays more rapidly but the difference in this example is not large; for example, Düchs'

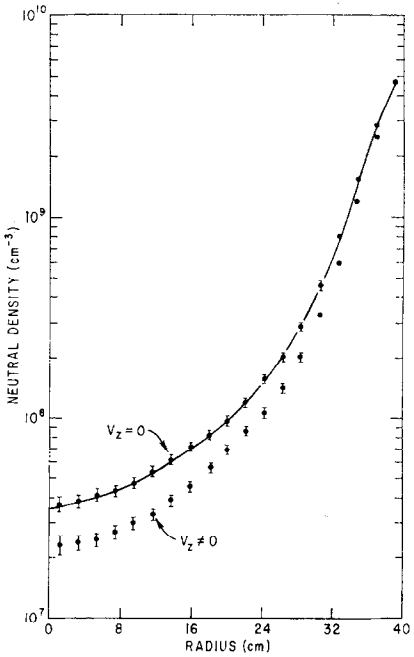

FIG. 5. Comparison with Düchs' model (——, Düchs' code; ⧳, Monte Carlo).

model overestimates the central neutral density by ~60%. This difference is simply due to the fact that, by constraining motion to the plane, path lengths are smaller and the attenuation is correspondingly reduced.

The neutral energy distributions obtained from both codes are in close agreement. However, Table 1 shows a large discrepancy in the flux of sputtered material. In our model this flux is reduced by a factor ~2 if we remove the $(\text{cosine})^{-1}$ dependence of the sputtering yield (which is not included in the Düchs code); the remaining difference is due to the different sputtering coefficients used in the two codes (see Fig.6).

TABLE I

Comparison of Particle Fluxes

	Neutral outflux (Γ_0 cm^{-2} sec^{-1})	Impurity influx (Γ_z cm^{-2} sec^{-1})	Γ_z/Γ_0
Düchs' code	6.24×10^{15}	3.79×10^{12}	6×10^{-4}
Monte Carlo	4.67×10^{15}	1.24×10^{13}	2.6×10^{-3}
		$(5.4 \times 10^{12})^a$	$(1.15 \times 10^{-3})^a$

[a] No angular dependence of sputtering coefficient.

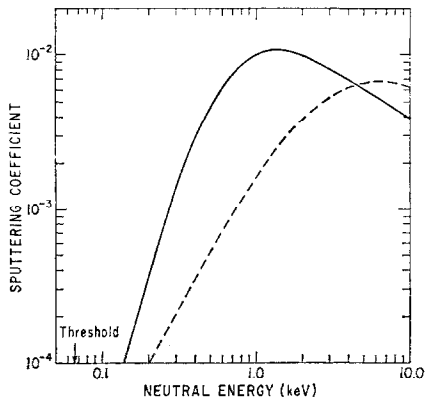

FIG. 6. Sputtering coefficients for H^+ incident on stainless steel. (——, from Ref. [8]; – – –, values used in Düchs' code).

The limited number of charge-exchange collisions allowed by Düchs' model means that, as the plasma thickness is increased, the neutrals will be unable to sample the entire ion-temperature distribution. This is illustrated in Fig. 7, which compares the neutral profiles when the plasma radius is increased to 85 cm. The discrepancy in the density distribution is similar to that in the previous case. However, there is now a substantial difference in the enrgy distributions in the central region of the plasma.

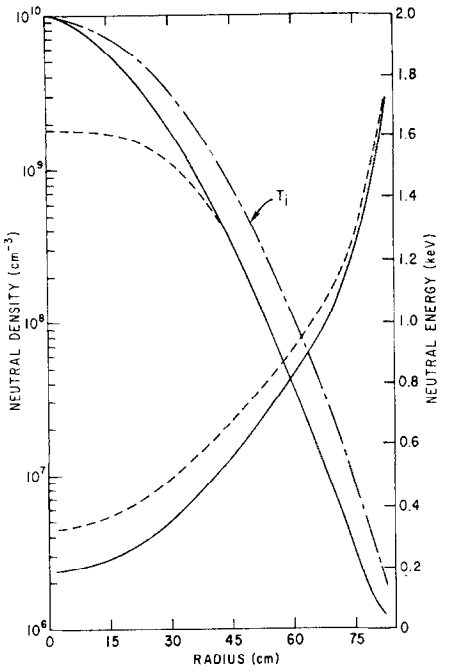

FIG. 7. Comparison with Düchs' model. (– – –, Düchs' code; ——, Monte Carlo).

3.2 *Charge-Exchange Spectra*

Measurements of the spectrum of charge-exchange neutrals is a widely used technique for measuring the ion temperature in tokamaks. The detector signal corresponding to some neutral energy ϵ is

$$s(\epsilon) \sim \int_0^l n_i \frac{e^{-\epsilon/T_i}}{T_i^{3/2}} \epsilon^{1/2} n_0 \overline{\sigma v}_{cx}(T_i, \epsilon)\, \eta\, dx \tag{3.20}$$

where the integral is evaluated along a chord to the detector and

$$\eta = \exp\left(-\int_0^x \frac{ds}{\lambda}\right)$$

is an attenuation factor with λ the total mean free path. Experimentally, it is assumed that if ϵ is sufficiently high, then the corresponding signal is due to charge exchange reactions at the point, s, along the chord where T_i is largest. In that case, if η and $\overline{\sigma v}_{\text{ex}}$ are independent of ϵ then a plot of $\ln[s(\epsilon)/\epsilon^{1/2}]$ as a function of ϵ should be linear with a slope equal to $-1/T_i(s)$.

To examine the validity of this experimental procedure we could, in principle, count those escaping particles which reach the detector. In general, however, Monte Carlo methods are not efficient in generating differential spectra since the number of ultimate results required is large. Instead, having determined the neutral density and

average energy distributions within the plasma we integrate (3.20) directly. A typical spectrum calculated in this way for PLT parameters is shown in Fig. 8. We calculate an ion temperature from this spectrum from a least-squares fit between $5T_i$ to $10T_i$, where T_i is the expected temperature. The ion-temperature distribution obtained by integrating (3.20) over a number of chords is compared with the actual distribution in Fig. 9. In this example, the discrepancy is $\leqslant 5\%$. If the temperature is measured from the slope between $2T_i$ and $4T_i$, then the error is increaed to $\leqslant 25\%$.

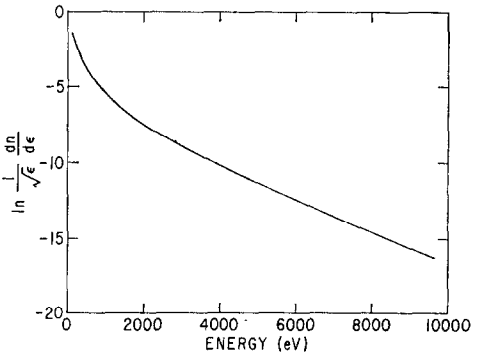

FIG. 8. Spectrum of charge exchange neutrals.

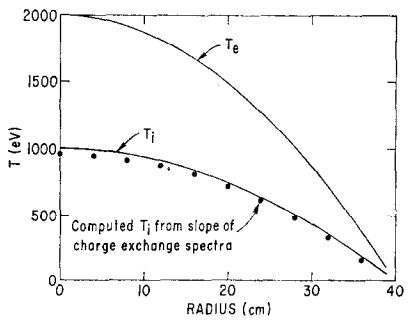

FIG. 9. Comparison of actual and measured temperatures.

4. SUMMARY

The Monte Carlo algorithm described here is accurate and economic. It competes favorably in running time with other schemes ($\sim$15–30 seconds of PDP-10 KI CPU time per profile). In addition, it has the advantage of being extremely flexible. Such items as volume sources and arbitrary boundary conditions (reflection, absorption, etc.) can easily be added. It also can be modified to allow the straightforward inclusion of such effects as charge exchange between O^+ and H° and H^+ and O°, and the calculation of mixtures of hydrogen such as D and T.

ACKNOWLEDGMENTS

The authors are grateful for the support and encouragement of Dr. Malvin Kalos of the Courant Institute of New York University, and to Dr. Paul Rutherford, Dr. Alan Boozer, Dr. Richard Smith, and Mr. Alan McKenney of the Princeton University Plasma Physics Laboratory for useful discussions.

This work was jointly supported by United States Energy Research and Development Administration Contract EY-76-C-02-3073 and by UKAEA, Culham Laboratory, Abingdon, United Kingdom.

REFERENCES

1. D. F. DÜCHS, *Bull. Amer. Phys. Soc.* (Oct. 1976), 1125.
2. E. GREENSPAN, *Nucl. Fusion* **14** (1974), 771.
3. L. L. CARTER AND E. D. CASHWELL, "Particle-Transport Simulation with the Monte Carlo Method," ERDA Critical Review Series, 1975.
4. M. H. KALOS, F. R. NAKACHE, AND J. CELNIK, "Computing Methods in Reactor Physics" (H. Greenspan, C. N. Kelber, and D. Okrent, Eds.), Chap. 5, Gordon & Breach, New York, 1968.
5. D. POST, *Bull. Amer. Phys. Soc.* (1976), 1108.
6. R. L. FREEMAN AND E. M. JONES, Culham Laboratory CLM-R 137 (1974).
7. A. C. RIVIERE, *Nucl. Fusion* **11** (1971), 363.
8. R. BEHRISCH, Summer School of Tokamak Reactors for Breakeven, Erice, 1976.
9. D. F. DÜCHS, D. E. POST, AND P. H. RUTHERFORD, "A Computer Model of Radial Transport in Tokamaks," *Nucl. Fusion* **17** (1977), 565.
10. D. DIMOCK, D. ECKHART, H. EUBANK, E. HINNOV, L. C. JOHNSON, E. MESERVEY, E. TOLNAS, AND D. J. GROVE, *in* "Proceedings of the Fourth International Conference of the IAEA, Madison, Wis., 1971," Vol. 1, p. 451.